UCRL- 93985
PREPRINT

THE HIGH PRESSURE EQUATION OF STATE OF LGP 1845 AND LGP 1846 (U)

Marc Costantino

This paper was prepared for submittal to the
1986 JANNAF Propulsion Meeing to be held in
New Orleans, LA August 26-28, 1986

August 4, 1986

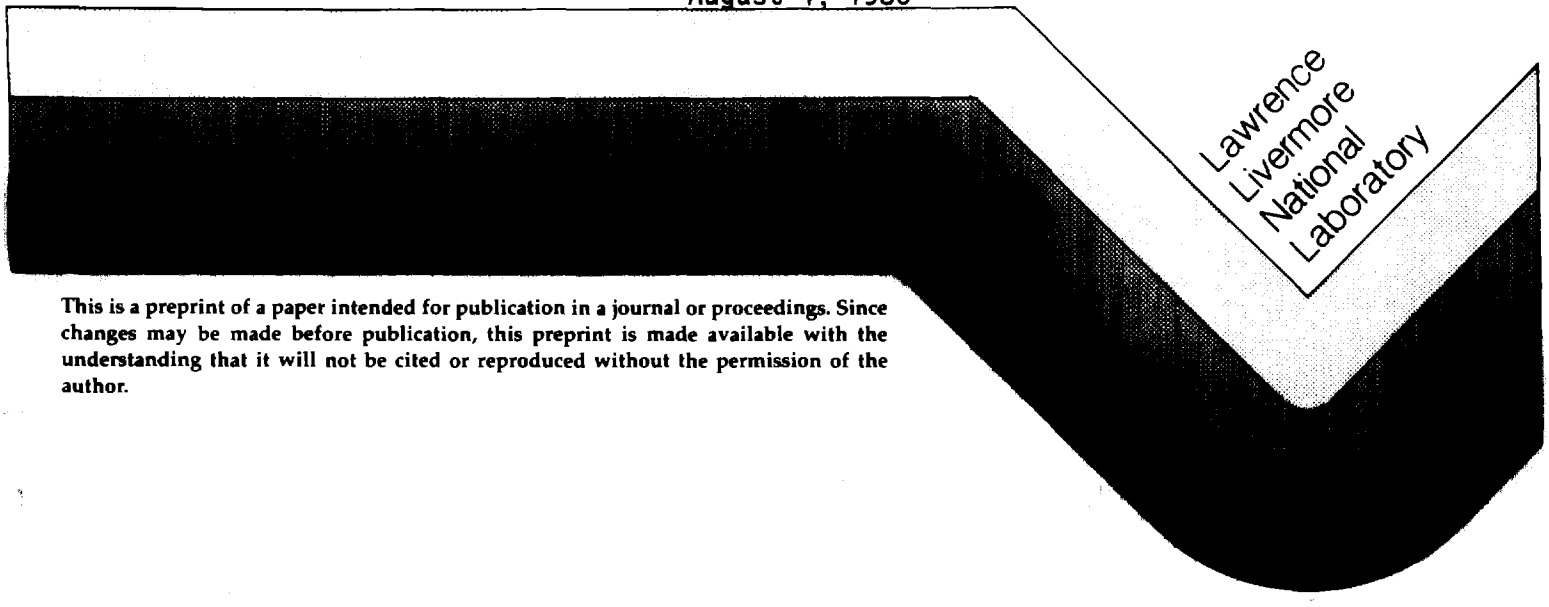

DISCLAIMER

THE HIGH PRESSURE EQUATION OF STATE OF LGP 1845 AND LGP 1846 (U)*

Marc Costantino
High Explosives Technology
Chemistry and Materials Science Department
Lawrence Livermore National Laboratory
Livermore, CA 94550

ABSTRACT

Compressible fluid dynamic and interior ballistic calculations of liquid gun propellants require the compressibility of the fluid as a function of pressure. I present isothermal and adiabatic compressibility data for the propellants LGP 1845 and 1846 at pressures to 500 MPa (72,500 PSI), at room temperature.

The isothermal and adiabatic compressibilities are measured simultaneously using a bellows piezometer having a fixed path arrangement for the compressional sound speed. Density as a function of pressure is obtained from the quasistatic compression of the propellant. Compressional sound speed at 1 MHz is measured using the pulse-echo-overlap technique, and the adiabatic compressibility is found from the sound speed and density. These data permit the calculation of the ratio of specific heats and the Gruneisen constant as a function of pressure.

The isothermal bulk modulus of these propellants increases from about 6 GPa at 0.1 MPa to about 16 GPa at 500 MPa. Over the same range, the sound speed increases from about 1940 to 2575 m/s; and the adiabatic bulk modulus from 5 to 10 GPa.

INTRODUCTION

A liquid gun propellant spends most of its time during the firing cycle at high pressure. This pressure varies from around a few MPa (1 MPa = 145 PSI) during the pumping-charging step to over 400 MPa during firing. Generally, calculations involving flow, mass conversion upon burning, and so forth, are linear in the density of the condensed phase. Additionally, the pressure in the gun chamber during the burn depends upon the difference between the chamber volume and the amount of unburnt liquid. Mechanical resonances ("pressure waves") are sensitive to the system geometry and the compression wave sound speed. Calculations for these problems must include the dependence of the density and the mechanical moduli on pressure. Assuming these quantities to be constant and equal to their value at 0.1 MPa leads to significant errors.

In this experiment, we measure simultaneously the isothermal and adiabatic compressibilities. We do this by using a classical bellows piezometer technique to find the absolute volume, V(P), of the liquid sample as a function of pressure and, at the same time, measure the compressional wave sound speed, $u_p(P)$. Knowing V(P) and $u_p(P)$, we can calculate the isothermal bulk modulus using $K_T = -V_o (\Delta P/\Delta V)_T$ and the adiabatic bulk modulus $K_S = \rho u_p^2$, where $\rho = \rho(P)$. We find that the moduli increase by almost a factor of three and the sound speed by about 30% over the 500 MPa pressure range.

EXPERIMENTAL

APPARATUS

The bellows piezometer technique for measuring the pressure-volume equation of state follows from Bridgman[1]. In this method, the liquid sample is placed in the bellows and the bellows inside a high pressure vessel. Since the spring constant of the bellows is negligible (in this work), the pressure in the sample is the same as in the pressure fluid. The volume of the sample at a given pressure is found by measuring the linear displacement of the bellows and using a calibration of bellows volume vs. length. We find the sound speed using the pulse-echo-overlap technique, in which we measure the time it takes for a sound pulse to make several round trips over a known distance. In the sections below we describe in detail the bellows piezometer and the sound speed measurement.

* Work performed under the auspices of the U.S. Department of Energy by the Lawrence Livermore National Laboratory under contract No. W-7405-ENG-48.

PIEZOMETER

Two piezometers were used in the course of this work. The first, having a bellows made of a nickel-copper-nickel laminate (Servometer Corp. Mdl FC-15) was destroyed after the first run. The LGP 1845 sample, left in the piezometer for six days awaiting a replicating run, ate through the bellows near a solder joint and escaped into the high pressure vessel, where its dessert consisted of the precision manganin gauge used to measure pressure, all of the high pressure feedthroughs, and part of the pressure vessel wall. The second piezometer employed a 304 stainless steel bellows (Metal Bellows Corp. Mdl 61230-2) welded to the threaded part of the body. Figure 1 is a sketch of the bellows piezometer. The tare consists of the bellows body, plug, and endcap. Attached to the top of the bellows body is a guide which fits closely, without binding, into the linear bearing pressed into the frame. The guide and bearing insure an axial displacement for the bellows as its internal volume changes. The guide also houses a BeCu wiper arm which forms the center tap of a linear potentiometer. The bellows body is fixed to the frame by means of set screws and its displacement with respect to the frame measured by the motion of the wiper arm along the fixed arm of the potentiometer, a 5 cm length of 30 gauge Tophet-A wire. The plug used to seal the open end of the bellows body also served as part of the structure used in the sound speed measurement, described below.

We find the absolute volume of the bellows at pressure, P, by measuring the voltages across the fixed and variable arms of the potentiometer to 1 microvolt, and using the calibration $V(P) = V_o + a_1R + a_2R^2$, where R is the ratio of the variable-to-fixed arm voltages. We determine the calibration coefficients, a_i, using the equation of state of water. In the calibration runs, we measure the pressure and calculate the volume of the water sample using

$$V_w(P) = V(P=0.1\text{MPa}, T)[1. + \rho_o(b_1\Delta P + b_2\Delta P^2 + b_3\Delta P^3)], \qquad (1)$$

where $\Delta P = P - 0.1$, ρ_o = density in gm/cm^3 at temperature T from Ref. 2, $b_1 = -4.4301(10^{-4})$, $b_2 = 5.8267(10^{-7})$, and $b_3 = -4.0699(10^{-10})$. Data, from Kennedy, et. al.,[3] for P < 110 MPa and from Burnham, et. al.,[4] for P > 110 MPa, were fitted to Eqn. 1 over the range 0-400 MPa, giving residuals of the order of 10^{-4} cm^3. The fitting parameters were used over the entire temperature range of the experiments (23°C < T < 26°C), since ignoring their change with temperature results in errors small compared to others in the experiment.

SOUND SPEED

We use the pulse-echo-overlap method[5] which, for materials that are not too lossy, gives excellent precision. In this method, a transducer launches a sound pulse which is reflected by an opposing surface at a known distance. The echo, in turn, is reflected at the transducer surface, creating a signal at the transducer. This process is repeated, resulting in a series of echoes having very similar phase structures. Two echoes are selected and, by means of time-delay circuitry, are overlapped by matching amplitudes and phases. We find the sound speed using

$$u_p = n\,\Delta x/\Delta t, \qquad (2)$$

where n is the number of echoes between those matched, Δx is the round trip travel path for one echo, and Δt the time delay required to overlap the two pulses. Note that, in this method, there is no requirement for the various corrections owing to system and travel path delays. (The phase change in the thin bond layer and stainless steel foil is negligible.) The precision of this method is better than 0.5%, even without taking great care.

The fixed travel path is formed by an assembly consisting of the sound transducer and a "cage." The transducer (from the Valpey-Fisher Co., .5" dia., 1MHz) is mounted on a .001" thick foil of 302A stainless steel using a silver paint and is damped by a mixture of tungsten powder and Scotchcast 221 (Fig. 1). Compression of the foil against the outside surface of the cage and the bellows body against its inside surface forms the seals preventing the pressure fluid and sample from mixing. We calculate the length of the travel path at 0.1 MPa using Eqn. 2 and data from Del Grosso and Mader[6]. Corrections for the change in travel path with pressure are negligible and ignored.

RESULTS

DATA REDUCTION

We calibrate the piezometer, check the internal consistency of the measurement technique and data reduction, estimate errors, and verify the sound speed method using published data for the P-v equation of state[3,4] and sound speed[6,9] for water. Comparison of measured values for $-(v-v_o)/v_o$ for water using the calibration Eqn. 2 with values calculated from Eqn. 1 shows that the precision of the data is about 0.4% in v/v_o and better than 5% in $\Delta v/v_o$. A similar comparison of the measured sound speeds with the data of Holton, et. al.,[9] indicates a precision of about 0.2%. Pressure is measured using a four-terminal manganin gauge, calibrated against a bourdon gauge having an accuracy of 0.3%.

Values for pressure and $-(v-v_o)/v_o$ for each run were smoothed using a cubic spline algorithm with four moveable knots. The isothermal bulk modulus was calculated at even pressure intervals by taking pointwise derivatives using interpolated volumes. The sound speed data are fitted adequately using a quadratic, which is used to interpolate between measured values. Next, using the smoothed volumes and interpolated sound speeds, we calculate the adiabatic bulk modulus. Finally, we find the ratio of specific heats, C_p/C_v from K_T/K_S.

LGP 1845 and LGP 1846

The formulation of these propellants are given in Table I. Data for LGP 1845 were taken in four independent runs. Three were replicated with the same sample loading to check for measurable degradation owing to pressure[7,8] (none was detected within the scatter of the data) and to provide an estimate of the experimental error. Two runs, each replicated once, were made for LGP 1846. We plot the P-v data as $-(v-v_o)/v_o$ in Fig. 2 for LGP 1845 and in Fig. 3 for LGP 1846 and list interpolated values at selected pressures in Tables II and III. The isothermal and adiabatic bulk moduli for LGP 1845 are plotted in Fig. 4 and in Fig. 5 for LGP 1846. We fit a quadratic to each set of data, mostly to aid the eye and to provide estimates for Tables II and III.

The fluid undergoes a compression of about 6% over 500 MPa, with the isothermal modulus increasing monotonically from about 6 to about 16 GPa and the adiabatic modulus from 5 to 10 GPa. The compressional sound speed data, also listed at selected pressures in Tables II and III, are shown in Fig. 6.

Using the density and compression sound speed at pressure P, we calculate the adiabatic bulk modulus, $K_S = \rho u^2$, and plot the results in Figs. 4 and 5. Finally, we calculate the ratio of specific heats, $\gamma = K_T/K_S$ and plot it in Fig. 7.

TABLE I. Compositions of LGP 1845 and LGP 1846

COMPONENT	LGP 1845	LGP 1846
water	16.81 (wt.%)	20.00
Hydroxylamine nitrate (HAN)	63.23	60.81
Triethanolaminenitrate (TEAN)	19.96	19.19

TABLE II. Summary of High Pressure Data for LGP 1845

P(MPa)	$-(v-v_o)/v_o$	K_T(GPa)	K_S(GPa)	u_p(m/s)	γ
0	0	5.82	5.53	1946	1.05
50	0.0085	6.63	6.03	2023	1.10
100	0.0161	6.88	6.53	2097	1.06
150	0.0232	7.37	7.02	2168	1.05
200	0.0296	8.13	7.51	2235	1.08
250	0.0355	9.13	8.00	2299	1.14
300	0.0407	10.02	8.48	2360	1.18
350	0.0455	11.13	8.94	2418	1.25
400	0.0498	12.68	9.39	2472	1.37
450	0.0535	13.81	9.82	2523	1.41
500	0.0568	14.22	10.23	2572	1.39

TABLE III. Summary of High Pressure Data for LGP 1846

P(MPa)	$-(v-v_o)/v_o$	K_T(GPa)	K_s(GPa)	u_p(m/s)	γ
0	0	6.52	5.30	1940	1.23
50	0.0097	6.39	5.78	2018	1.11
100	0.0186	6.77	6.26	2092	1.08
150	0.0231	7.27	6.73	2163	1.08
200	0.0297	7.93	7.21	2232	1.10
250	0.0357	8.78	7.67	2297	1.14
300	0.0410	10.05	8.13	2359	1.23
350	0.0456	11.45	8.58	2417	1.34
400	0.0497	13.29	9.00	2473	1.47
450	0.0531	15.84	9.41	2526	1.68
500	0.0562	17.92	9.82	2575	1.83

DISCUSSION

The liquid propellants 1845 and 1846 are quite similar in their high pressure mechanical properties. Within experimental error, the isothermal bulk moduli are the same, increasing from about 6 to about 16 GPa over 500 MPa. Using a linear interpolation for intermediate pressures certainly is acceptable, although the P-v curve is softer at lower pressures. The fitted quadratics are (K_T is in GPa and P in MPa):

$$K_T = 6.13 + 4.16(10^{-3})\ P + 3.03(10^{-5})\ P^2$$

for 1845 and 1846 data, combined (standard deviation is 1.4 GPa);

$$K_T = 5.87 + 8.65(10^{-3})\ P + 1.82(10^{-5})\ P^2$$

for LGP 1845; and

$$K_T = 6.59 - 4.83(10^{-3})\ P + 5.51(10^{-5})\ P^2$$

for LGP 1846. Since $\Delta V = V_o \frac{\Delta P}{K_T}$, the volume at P is sensitive to the relatively large change in K_T.

Similar comments apply to the adiabatic moduli, although there is no statistical difference between the linear and quadratic fitted curves. The linear curves are

$$K_s = 5.51 + 9.37(10^{-3})\ P$$

for LGP 1845 and LGP 1846 combined,

$$K_s = 5.60 + 9.45(10^{-3})\ P$$

for LGP 1845, and

$$K_s = 5.35 + 9.11(10^{-3})\ P$$

for LGP 1846. Each fitted curve has a standard deviation of less than 0.2 GPa.

Compressional sound speeds for the two formulations are indistinguishable. Again, values may be estimated using a linear interpolation, although the quadratics

$$u_p = 1946 + 1.674\ P - 6.46(10^{-4})\ P^2$$

for LGP 1845 (standard deviation of the fit is 17 m/s for all data); and

$$u_p = 1940 + 1.582\ P - 6.22(10^{-4})\ P^2$$

for LGP 1846 (standard deviation is 6 m/s) are justifiable. Based on the reproducibility between replicate runs, there is no pressure induced mechanical degradation of these materials.

Mechanical resonances at frequencies above 10 kHz are a serious concern, since the wavelength of such a pressure disturbance is of the order of millimeters to centimeters. These data make it possible to evaluate the susceptibility of a proposed geometry to standing waves over the pressure range of the ballistic cycle.

Finally, although it is somewhat presumptuous with the present data, we calculate the ratio of specific heats, $\gamma = K_T/K_s = C_p/C_s$. We do this since, with the addition of an ambient pressure measurement of the thermal expansion, all of the thermodynamic properties of the liquid can be estimated for pressures of the ballistic cycle. The data are good enough to show $\gamma > 1$ and to increase with pressure, as expected. For all data,

$$\gamma = 1.11 - 6.94(10^{-4})\ P + 3.27(10^{-6})\ P^2$$

for LGP 1845 and LGP 1846 combined, with a standard deviation of 0.16.

The density (or specific volume) of a solid or liquid gun propellant is a first order quantity in interior ballistics calculations. Errors made by assuming the density to be constant over the pressures of the ballistic cycle propagate linearly and may be as large as several per cent for propellants having little porosity and larger for those more porous. These errors occur in two important parts of the calculation. First, the macroscopic volume available to the product gases, and hence the pressure, is a function of the unreacted condensed phase. Assuming this phase to be incompressible results in errors in the gas volume of several per cent (depending on the loading density), which can be reduced significantly by using even an estimate for the compressibility. While it is true that the size of the error is proportional to the total amount of solid material, which is greatest during the low pressure, early, part of the cycle; the error still is appreciable during later times. The second important error made in assuming an incompressible solid phase is in the mass generation rate. For a given surface regression rate at some pressure, P, the mass generation is proportional to $\rho(P)$. Using a density determined at P = 0.1 MPa results in errors in mass generation rates at pressure P equal to the volume compression at P. For the liquid propellants studied in this work, this amounts to about 5% at 400 MPa. While these errors cannot be ignored, they can be reduced to second order by simply making a guess at the compressibilities. Of course, laboratory data for the material at hand are preferable, although estimates from a data base of similar materials probably are acceptable.

REFERENCES

1. Bridgman, P. W., "The Volume of Eighteen Liquids as a Function of Pressure and Temperature," Proc Amer Acad Arts Sci, 66, 185(1931); and Bridgman, P. W., "The Pressure-Volume-Temperature relations of the liquid and the phase diagram of heavy water," J Chem Phys, 3, 597(1935).

2. Handbook of Chemistry and Physics, 41st Ed., pg 2129.

3. Kennedy, G. C., W. L. Knight, and W. T. Holser, "Properties of Water. Part III. Specific Volume of Liquid Water to 100°C and 1400 Bars," Am J Sci, 256, 590(1968).

4. Burnham, C. Wayne, John R. Holloway, and Nicholas F. Davis, "Thermodynamic Properties of Water to 1,000°C and 10,000 Bars," The Geological Society of America Special Paper Number 132, 1969.

5. Papadakis, Emmanuel P., "Ultrasonic Phase Velocity by the Pulse-Echo-Overlap Method Incorporating Diffraction Phase Corrections," J Acoust Soc Amer 42, 1045(1967).

6. Del Grosso, V. A. and C. W. Mader, "Speed of Sound in Pure Water," J Acoust Soc Amer 52, 1442(1972).

7. Van Dijk, C. A. and R. G. Priest, "Thermal Decomposition of Hydroxylammonium Nitrate at Kilobar Pressures," Combustion and Flame 57, 15-24(1984).

8. Fifer, R. A., L. J. Decker, and P. J. Duff, "DSC Stability Test for Liquid Propellants," 22d JANNAF Combustion Meeting, 7-10 October 1985. Jet Propulsion Laboratory, Pasadena, CA.

9. Holton, Gerald, M. Paul Hagelberg, Samuel Kao, and Walter H. Johnson, Jr., "Ultrasonic-Velocity Measurements in Water at Pressures to 10,000 kg/cm^2," J. Acoust. Soc. Amer., 43, 102(1968)

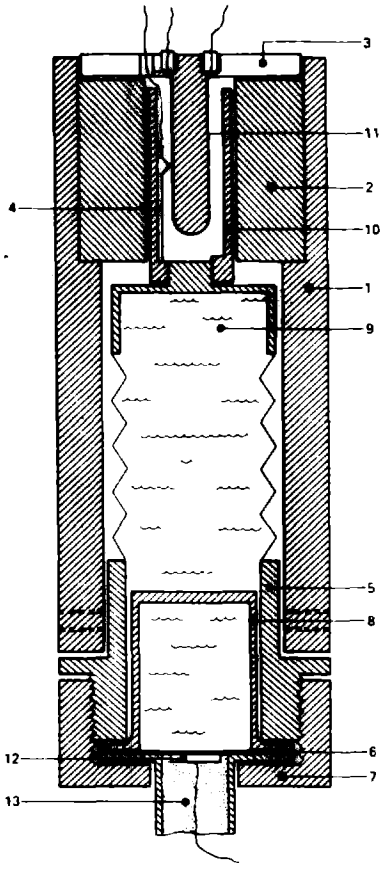

Fig. 1 Bellows piezometer. 1. Frame; 2. Linear bearing; 3. Linear Potentiometer fixed arm assembly; 4. BeCu wiper; 5. bellows body; 6. stainless steel diaphragm; 7. endcap; 8. sound cage; 9. liquid sample; 10. guide; 11. wire, forming the fixed arm of the potentiometer; 12. PZT-5 transducer; 13. espoxy/tungsten powder damping medium.

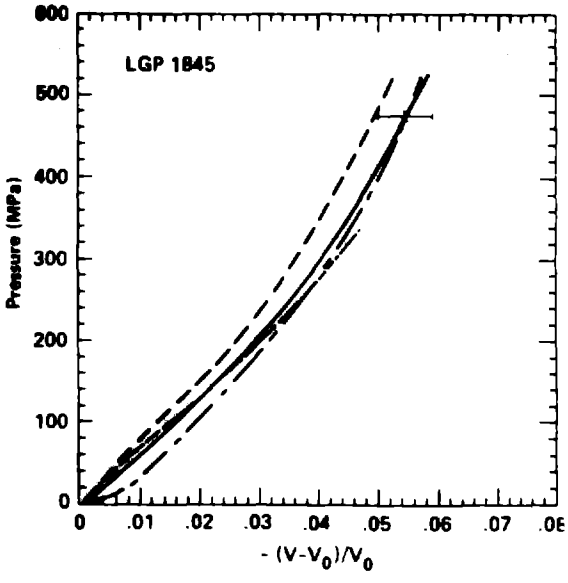

Fig. 2 $-(v/v_o)/v_o$ vs. pressure for LGP 1845. The solid curve is the average of several values at each pressure, from the data in Table II.

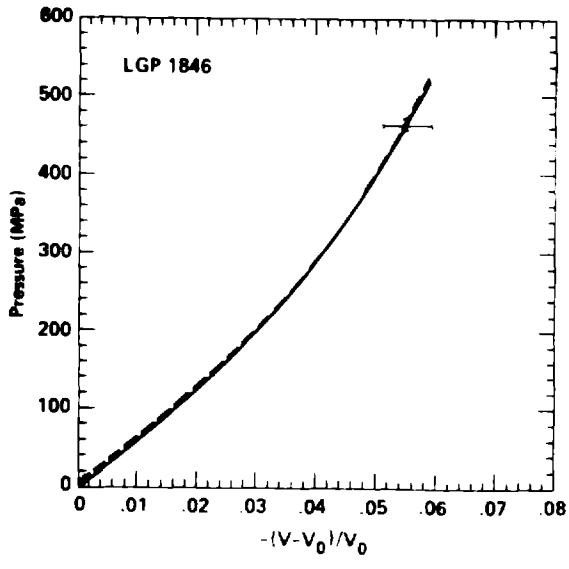

Fig. 3 $-(v/v_o)/v_o$ vs. pressure for LGP 1846. The solid curve is the average of several values at each pressure, from the data in Table III.

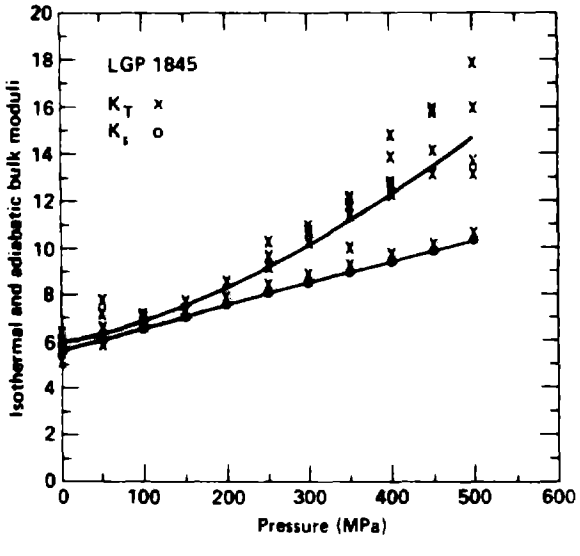

Fig. 4 Isothermal (x) and adiabatic (o) bulk modulus vs. pressure for LGP 1845.

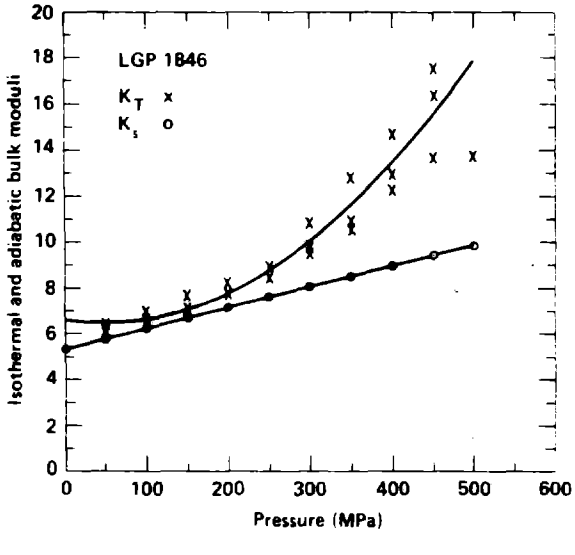

Fig 5 Isothermal (x) and adiabatic (o) bulk modulus vs. pressure for LGP 1846.

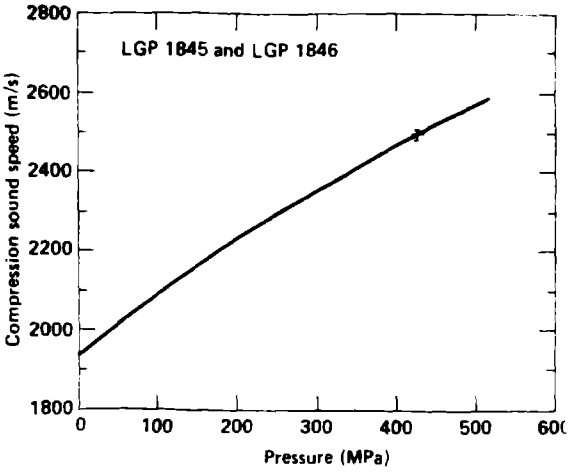

Fig. 6 Compression sound speed vs. pressure for LGP 1845 and LGP 1846. Each curve is the average of several runs, with a standard deviation of about 1%.

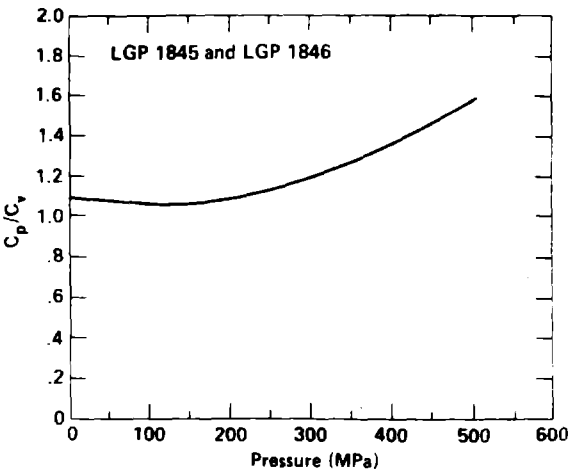

Fig. 7 Ratio of specific heats, $\gamma = K_T/K_S$, for LGP 1845 and LGP 1846.